Biochimica et Biophysica Acta 1783 (2008) 1972–1980

Contents lists available at ScienceDirect

Biochimica et Biophysica Acta

journal homepage: www.elsevier.com/locate/bbamcr

Differential subnuclear localisation of hnRNPs A/B is dependent on transcription and cell cycle stage

Lexie R. Friend, Siew Ping Han, Joseph A. Rothnagel, Ross Smith *

School of Molecular and Microbial Sciences, The University of Queensland, Brisbane, Queensland 4072, Australia

ARTICLE INFO

Article history:
Received 12 March 2008
Received in revised form 23 May 2008
Accepted 23 May 2008
Available online 6 June 2008

Keywords:
hnRNP A/B
Spliceosome
Splicing factor
Transcription inhibition
Immunoprecipitation
Cell cycle

ABSTRACT

The heterogeneous nuclear ribonucleoproteins A1, A2/B1 and A3 (hnRNPs A/B) are involved in many nuclear functions that are confined to distinct regions within the nucleus. To characterise and compare the distribution of the hnRNPs A/B in these subnuclear compartments, their colocalisation with spliceosomal components, nascent transcripts and other nuclear markers in HeLa cells was investigated by immunostaining and transfection of GFP constructs. The mechanisms of this localisation were further explored by treating cells with detergent, nucleases and transcription inhibitors. We have also examined the dynamics of A2/B1 throughout the cell cycle. Our results show that hnRNPs A/B have different subnuclear localisations, with A1 differentially localised to the nuclear envelope, and A2/B1 and A3 enriched around nucleoli. This pattern of distribution was dependent on RNA integrity and active transcription. The hnRNPs A/B preferentially colocalised with a subset of splicing factors. Significantly, only rarely did transcription factories colocalise with high levels of these hnRNPs. Moreover, localisation of A2/B1 changed with cell cycle stage. Our findings show that the subnuclear localisation of the hnRNPs A/B is differentially, spatially and temporally regulated, and suggest that this localisation may be relevant to their nuclear functions.

1. Introduction

The heterogeneous nuclear ribonucleoprotein (hnRNP) A/B family of proteins is comprised of A1, A2/B1, A3 and A0. These multifunctional proteins have a wide range of roles in diverse cellular events, including RNA processing and trafficking [1], cell senescence [2], translational regulation [3], cell cycle regulation [4], stress response [5] and miRNA processing [6]. Within the nucleus, aside from their well-recognised role in packaging nascent RNA, the hnRNPs A/B may also be involved in splice site selection [7,8], transcription regulation [9], telomere maintenance [10–13], DNA replication [14] and splicing regulation [15–19].

While much information is available about the activity of the hnRNPs A/B in the nucleus, in particular for A1 and A2/B1, less is known about the localisation of these proteins in subnuclear compartments. A1 and A2/B1 have been found in nucleolar preparations, along with other splicing factors such as U2AF [20]. However, as it is possible that subcellular fractionation procedures may disrupt normal cellular organisation and produce artifacts, localisation validation by a variety of methods is necessary for confirmation of these findings [21]. Several studies [22,23] employing fluorescent immunostaining methods have shown that the hnRNPs A/B display widespread nucleoplasmic staining that is excluded from nucleoli, but due to the overwhelming abundance of these proteins in the nucleus further details were not discernable. While the hnRNPs A/B have consistently been isolated in most, but not all, stages of spliceosomal assembly [24–29], these studies have been conducted *in vitro* and require further investigation for their findings to be extended to the situation *in vivo*.

Most nuclear processes, including RNA processing, transcription and DNA replication, are organised spatially and temporally [30]. Three of the most prominent subnuclear structures are nucleoli, Cajal bodies and splicing speckles or splicing factor compartments, which have different structural and functional properties [31]. For example, newly assembled small nuclear ribonucleoproteins (snRNPs) are imported from the cytoplasm into the nucleus where they first localise transiently in Cajal bodies and undergo modification. The snRNPs then accumulate in splicing factor compartments before recruitment to active sites of transcription [32–34]. In addition, DNA replication and transcription occur at defined nuclear sites known as replication factories and transcription factories [35,36]. Thus, in this highly dynamic and intricately compartmentalised environment, detailed *in vivo* characterisation of subnuclear localisation is essential to advance our understanding of the function of nuclear proteins such as the hnRNPs A/B.

In the present study, we have investigated the colocalisation of hnRNPs A1, A2/B1 and A3 with spliceosomal and other nuclear components in fixed and living cells. We show that although they are

Abbreviations: hnRNPs, heterogeneous nuclear ribonuclear proteins; RRM, RNA recognition motif; snRNPs, small nuclear ribonuclear proteins

* Corresponding author. Tel.: +61 7 3365 4627; fax: +61 7 3365 4699.
E-mail address: ross.s@uq.edu.au (R. Smith).

0167-4889/$ – see front matter © 2008 Elsevier B.V. All rights reserved.
doi:10.1016/j.bbamcr.2008.05.021

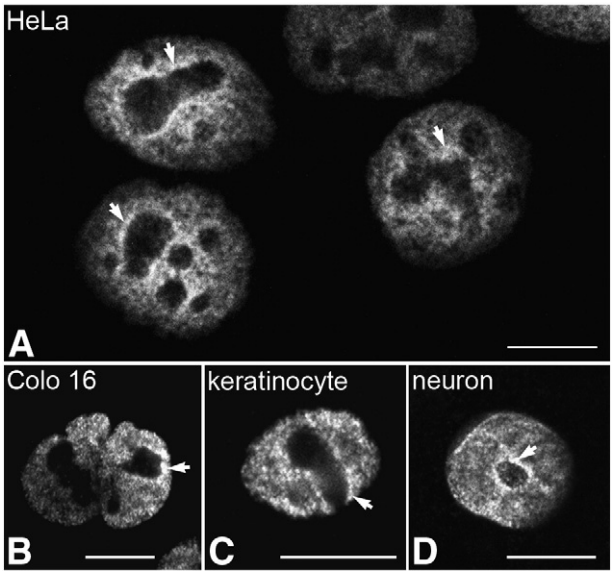

Fig. 1. Subnuclear localisation of A2/B1 in (A) HeLa cells, (B) Colo16 cells, (C) primary keratinocytes and (D) hippocampal progenitor cells. Fixed cells were immunostained using a rabbit polyclonal antibody against A2/B1, followed by an anti-rabbit Alexafluor-488-conjugated secondary antibody, and imaged using confocal microscopy. Arrows point to enriched regions of A2/B1 surrounding the nucleoli. Bar, 10 μm.

closely related paralogues, the distribution of A1 in the nucleus is markedly different from that of A2 and A3. A1 preferentially localises at the nuclear envelope, whereas A2 and A3 concentrate in the perinucleolar region. These features were highlighted by detergent-mediated removal of the diffuse nucleoplasmic proteins. Treatment with RNase A or transcription inhibitors perturbed this localisation, demonstrating its dependence on interactions with RNA. Some spliceosomal components ($U2AF^{65}$, snRNAs and Sm proteins) spatially overlapped with A2/B1 whereas others (SC-35) did not, suggesting that the hnRNPs A/B may associate preferentially with a subset of the spliceosomal complexes. High levels of hnRNPs A/B were associated only infrequently with nascent transcripts, suggesting a temporal separation between pre-mRNA synthesis and its association with these proteins. Finally, cell cycle studies revealed that the perinucleolar concentration of A2/B1 seen in interphase was disrupted in early mitosis.

2. Materials and methods

2.1. Cell culture

HeLa cells were maintained in DMEM (Gibco, Victoria, Australia) containing 10% newborn calf serum, 100 U/ml penicillin, 100 μg/ml streptomycin, HEPES, pH 7.4 at 37 °C in a humidified 5% CO_2 atmosphere.

2.2. Antibodies

Rabbit polyclonal antibodies directed against A1 (1:40), A2/B1 (1:200) and the N-terminal of A3 (1:500) were raised in our laboratory [37]. The specificity of these antibodies was confirmed by peptide blocking experiments. The following mouse monoclonal antibodies were also used in this study: anti-hnRNP A1, Clone 4B10 (Sigma, Sydney, Australia; 1:1000), anti-SC-35 (Sigma, 1:2000), anti-Sm (Y12) (AbCam, Cambridge, UK; 1:100), anti-2,2,7-trimethylguanosine (anti-TMG) (Calbiochem,

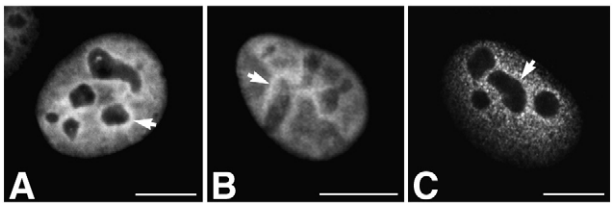

Fig. 2. The perinucleolar localisation of A2/B1 was verified using several methods. (A) HeLa cell fixed 16 h after transfection with A2-GFP plasmid DNA. (B) Live B104 cell imaged 4 h after microinjection with A2-GFP plasmid DNA. (C) HeLa cell that was detergent extracted with 0.2% Triton X-100/CSK buffer for 5 min prior to fixation, then fixed and immunostained for A2/B1 followed by Alexafluor-488-conjugated secondary antibody. Arrows point to enriched regions of A2/B1 surrounding the nucleoli. Bar, 10 μm.

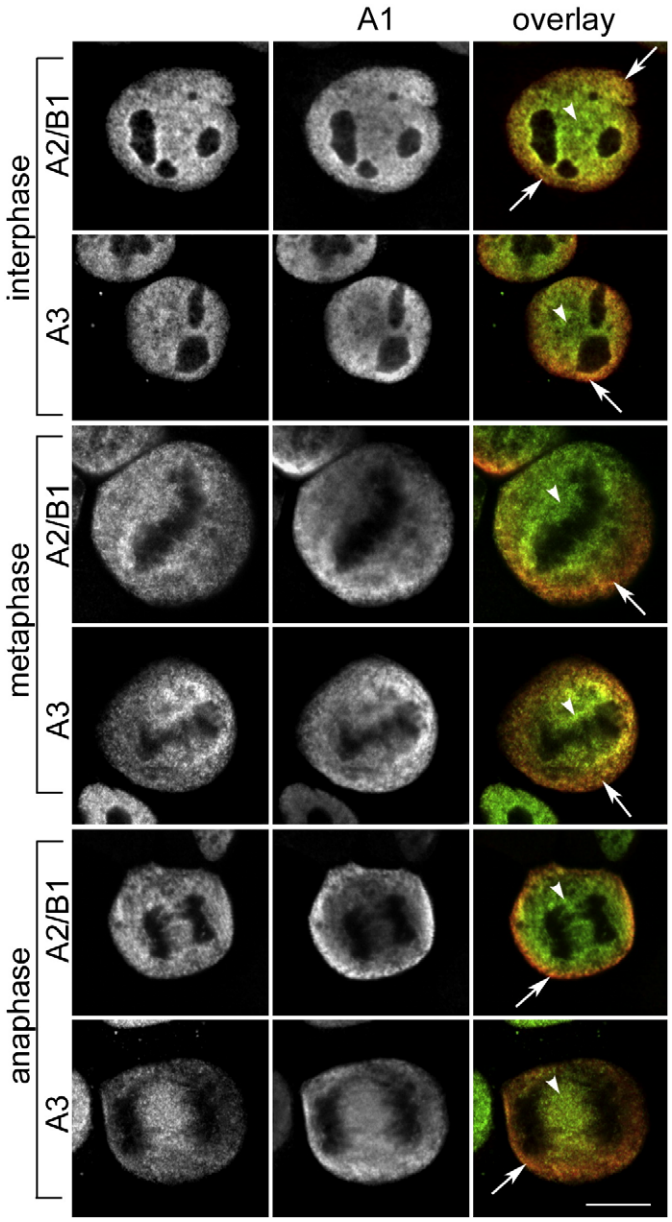

Fig. 3. Differential subnuclear distribution of hnRNPs A/B. HeLa cells in interphase, metaphase and anaphase were fixed and double-labelled with a mouse monoclonal antibody against A1 followed by anti-mouse Alexafluor-546-conjugated secondary antibody, (middle column, red in overlay) and rabbit polyclonal antibodies against A2/B1 or A3 followed by anti-rabbit Alexafluor-488-conjugated secondary antibody (left column, green in overlay). Cells were then imaged using confocal microscopy. Arrows point to the regions enriched for A1 only, while arrowheads point to the regions enriched for A2/B1 or A3 only. Bar, 10 μm.

Victoria, Australia; 1:400 for immunofluorescence), anti-U2AF^{65} (Sigma, 1:3000) and anti-bromodeoxyuridine (anti-BrdU) (Chemicon, Sydney, Australia; 1:50). The following secondary antibodies were all from Molecular Probes (Victoria, Australia): Alexa 488 goat anti-mouse (1:1000), Alexa 546 goat anti-mouse (1:3000), Alexa 488 goat anti-rabbit (1:1000) and Alexa 546 goat anti-mouse (1:3000).

2.3. Immunocytochemistry

HeLa cells were grown on 12 mm glass coverslips to ~60% confluency, after which cells were fixed in 4% paraformaldehyde (PFA)/phosphate-buffered saline (PBS) for 10 min and permeabilised with 0.1% Triton X-100/PBS for 10 min, both at room temperature. In some cases, detergent extraction was performed on live cells prior to immunostaining. As well, a range of concentrations of Triton X-100 (0.05–10%) in PHEM buffer (60 mM PIPES, 25 mM HEPES, 20 mM EGTA, 1 mM $MgCl_2$, pH 7.4 with KOH) was tested on GFP-transfected HeLa cells, and the optimal concentration (0.2%) was used for subsequent experiments. Following permeabilisation or detergent extraction, cells were immunostained using the appropriate primary and secondary antibodies. Images were then acquired on a laser-scanning confocal microscope (LSM 510 Meta, Zeiss Inc., Oberkochen, Germany). Other cell types were processed in the same manner.

2.4. Transient transfection assays

GFP-tagged constructs of nuclear markers B23, H2B, coilin, and SMN were propagated in DH5α cells. To generate A2-GFP, PCR was performed on mouse skin cDNA using a forward primer to introduce an XhoI site and Kozac sequence, and a reverse primer to introduce an AgeI site flanking the hnRNP A2 sequence. The amplified product was gel-extracted, ligated into pGemT-Easy Vector and electroporated into DH5α cells. Positive clones were digested with XhoI and AgeI, and the insert was subcloned into pEGFP-N1 (Clontech, CA). The resulting plasmid was propagated in Stbl2 cells (Invitrogen, Victoria, Australia). HeLa cells grown in 24-well plates were transfected with 200 ng of plasmid DNA per well using Fugene 6 (Roche, Sydney, Australia), and fixed 16 h post-transfection. B104 cells were imaged 4 h after microinjection of 100 ng of A2-GFP plasmid DNA.

2.5. Nuclease digestion of living cells

Nuclease digestion was performed as previously described [38]. HeLa cells grown overnight on coverslips were extracted in 0.2% Triton X-100 in CSK buffer (100 mM NaCl, 300 mM sucrose, 10 mM PIPES at pH 7.4, 3 mM $MgCl_2$, 1 mM EGTA, 1 mM PMSF) for 5 min at room temperature. The cells were treated with either 100 μg/ml RNase A (Fermentas, Ontario, Canada) in CSK buffer for 10 min at 37 °C, or 100 μg/ml DNase 1 (Worthington, NJ) in PBS with 5 mM $MgCl_2$ for 20 min at room temperature. Then, cells were fixed and processed as for immunostaining. In addition, cells were stained with Hoechst 32258 Dye (Molecular Probes, 1:10,000) in PBS for 5 min to monitor DNA levels, and some coverslips were also incubated for 5 s in Pyronin Y Dye (Sigma, 1:15,000) to monitor RNA levels.

2.6. Transcription inhibition

HeLa cells were grown overnight on coverslips and treated the following day with 5 μg/ml actinomycin D (Sigma) for 1–3 h or 50 μg/ml α-amanitin (Sigma) for 5 h, both at 37 °C.

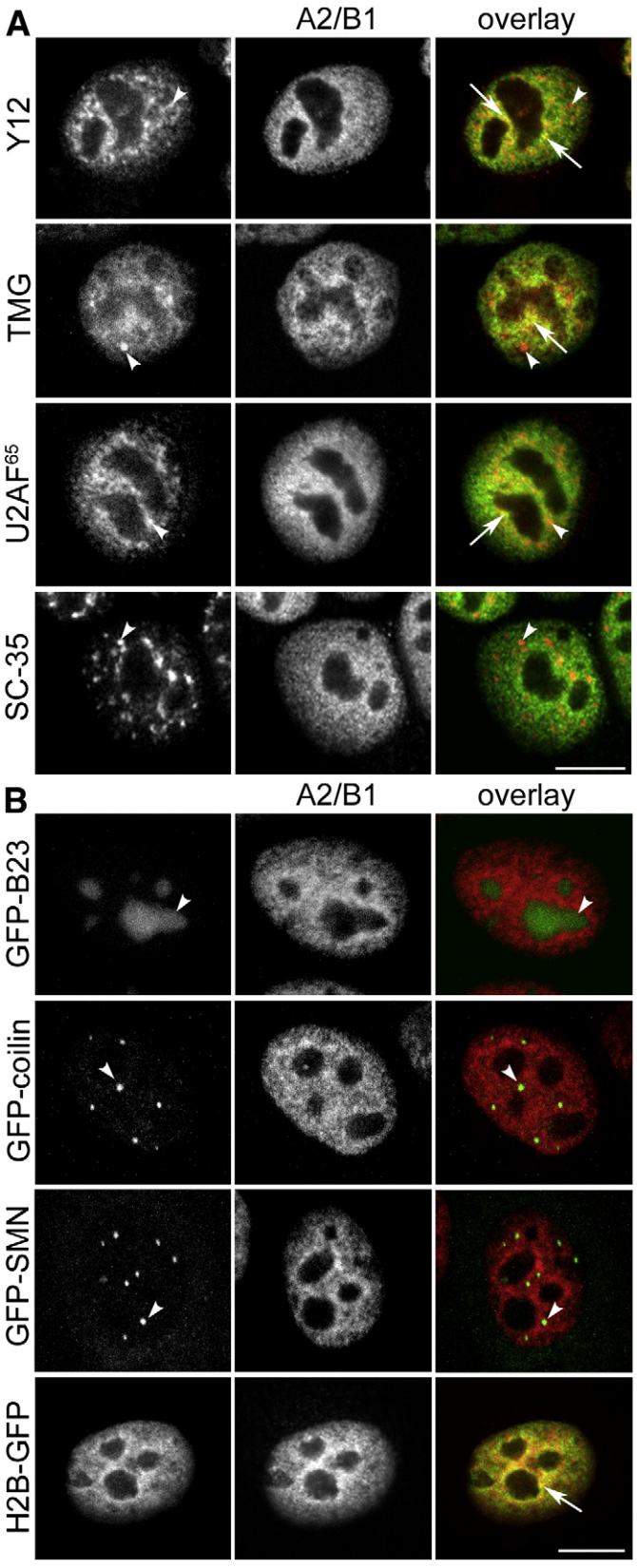

Fig. 4. Comparison of A2/B1 subnuclear distribution with nuclear markers. (A) HeLa cells were double-labelled with mouse monoclonal antibodies against splicing factors followed by anti-mouse Alexafluor-546-conjugated secondary antibody, (left column, red in overlay) and rabbit polyclonal antibody against A2/B1 followed by anti-rabbit Alexafluor-488-conjugated secondary antibody (middle column, green in overlay). (B) HeLa cells were transfected with GFP-tagged markers (left column, green in overlay) for various subnuclear compartments and immunostained for A2/B1 followed by Alexafluor-546-conjugated secondary antibody (middle column, red in overlay). Cells were then imaged using confocal microscopy. Arrows point to the regions of colocalisation, while arrowheads point to the regions enriched for either the red or green signal only. Bar, 10 μm.

Cells were then fixed, immunostained and stained for nucleic acids as described earlier. Images were collected using confocal microscopy with the same microscope settings used for every time point tested.

2.7. BrUTP labelling

For BrUTP labelling, a variation of the method presented in Andersen et al. [39] was used. HeLa cells were grown overnight on coverslips, permeabilised, and preincubated in physiological buffer (PB) (100 mM KOAc, 30 mM KCl, 10 mM Na_2HPO_4, 1 mM $MgCl_2$, 1 mM Na_2ATP, 1 mM DTT, 0.2 mM PMSF and 80 U/ml RNAsin) at 33 °C for 2 min. They were then incubated in transcription mix (1 mM ATP, 0.1 mM GTP, 0.1 mM CTP, 0.1 mM BrUTP, 1 mM $MgCl_2$ in PB) at 33 °C for 15 min. Cells were then washed, permeabilised on ice, fixed and immunostained for BrdU and the hnRNPs A/B, after which they were imaged using confocal microscopy. To confirm that our results were not method-dependent, cells were also labelled with BrUTP by another method [40]. For this method a range of conditions including duration of labelling and detergent concentrations, was used. Both methods gave comparable results.

2.8. Cell cycle synchronisation

HeLa cells were synchronised using the mitotic shake-off method [41]. Mitotic cells were obtained by vigorously shaking an asynchronously growing cell population for 1 min in 5 ml of medium. These cells were then plated onto fibronectin-coated coverslips (5 μg/50 μl) at a density of ~1.6×10^5 and ~9.0×10^3 cells/well for flow cytometry (FACS) and immunostaining, respectively. At 2 h intervals, cells for FACS were harvested by trypsinisation, fixed in 70% ethanol and the DNA stained with propidium iodide (25 μg/ml) containing RNase A (100 μg/ml). At the same time points, cells for immunofluorescence microscopy were fixed in 4% PFA/PBS, immunostained and the DNA stained using Hoechst 32258 Dye. Cell synchrony of the mitotic population was monitored by FACS analysis of the propidium iodide-stained cells. Cells for immunofluorescence studies were assigned cell cycle stage based on the DNA content of the cells collected at each time point. The data obtained from FACS analysis were gated to exclude small cellular debris and clumps or multiples of cells.

3. Results

3.1. Different hnRNPs A/B are localised in overlapping but distinct regions within the nucleoplasm

In HeLa cells, A2/B1 displayed widespread nucleoplasmic immunostaining that was enriched around nucleoli but excluded from them (Fig. 1A, short arrows), in accord with previous studies [22]. Similar staining features were evident in other cell types, including Colo16 (a keratinocyte cell line) [42], primary proliferating human keratinocytes and hippocampal progenitor cells (Fig. 1B–D). Thus, this pattern of localisation was not cell-type dependent since it was present in simple epithelial (HeLa), stratified epidermal (Colo16 and primary keratinocytes) and neuronal (hippocampal) cells.

Similar localisation patterns were obtained using other experimental approaches. Transfection and microinjection of A2-GFP constructs into HeLa cells and B104 neuroblastoma cells, respectively, produced a fluorescence pattern similar to that of immunostaining of endogenous proteins, with enrichment of signal around nucleoli (Fig. 2A,B). This pattern was evident in both fixed (Fig. 2A) and living cells (Fig. 2B). In addition, detergent extraction was performed prior to fixation of living cells, in order to remove soluble proteins. The enrichment of A2/B1 around nucleoli persisted under these conditions (Fig. 2C), demonstrating that these local concentrations are maintained by stable interactions with detergent-resistant components. Indeed, a large pool of hnRNPs was still present in the cells after extraction with the highest concentration of detergent tested (10%) (data not shown).

Differences between the immunostaining patterns of A1, A2/B1 and A3 were observed. The A1 signal was concentrated at the nuclear envelope of most cells (Fig. 3, arrows), and diminished in the centre of

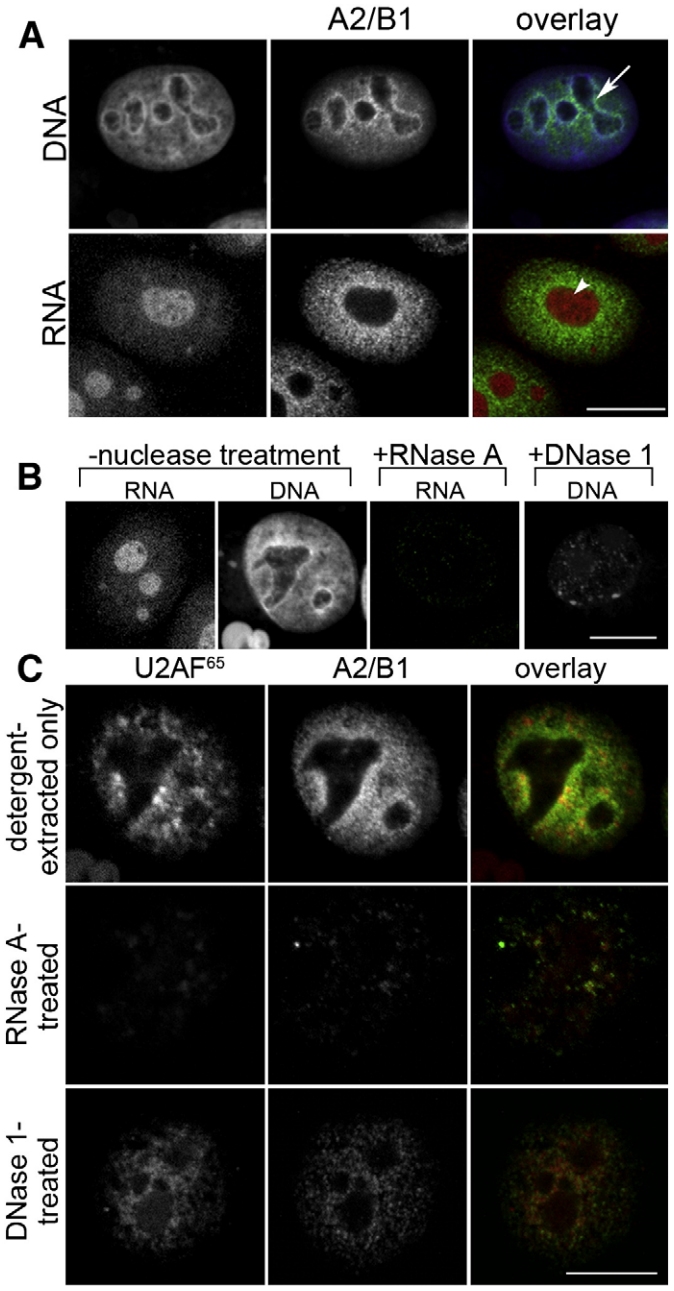

Fig. 5. Interaction of A2/B1 with nucleic acids. (A) HeLa cells were immunostained for A2/B1 followed by Alexafluor-488-conjugated secondary antibody (middle column, green in overlay), and then stained for DNA using Hoechst Dye (left, blue in overlay) or RNA using Pyronin Y Dye (left, red in overlay). The arrow points to a region of colocalisation, while the arrowhead points to a region enriched for the red signal only. (B) HeLa cells were extracted with 0.2% Triton X-100/CSK buffer for 5 min, followed by treatment with 100 μg/ml RNase A or 100 μg/ml DNase 1. Cells were then fixed and stained for RNA and DNA using Pyronin Y Dye and Hoechst Dye, respectively. The concentrations of RNase and DNase used almost completely removed RNA and DNA, respectively. (C) HeLa cells were treated using the same conditions as in (B). Control cells were extracted with detergent, but without nuclease treatment. Cells were then fixed and immunostained for A2/B1 followed by Alexafluor-488-conjugated secondary antibody (middle column, green in overlay) and $U2AF^{65}$ followed by Alexafluor-546-conjugated secondary antibody (left column, red in overlay). Images were taken using confocal microscopy at constant settings. The brightness and contrast of the overlaid image for the RNase A-treated cells have been adjusted to visualise the signals for A2/B1 and $U2AF^{65}$. Bar, 10 μm.

the nucleus. In contrast, A2/B1 and A3 were present throughout the nucleoplasm (Fig. 3, arrowheads). Thus, a distinctive "border" was produced when the A1 signal was overlaid on that of A2/B1 or A3 (Fig. 3, overlays). Interestingly, this pattern was maintained in cells undergoing metaphase and anaphase. This may represent a redistribution of A1 into the endoplasmic reticulum network, which remains intact as the nuclear envelope disassembles during mitosis [43].

3.2. Colocalisation of hnRNP A2/B1 with spliceosomal and other nuclear proteins

To further characterise the distribution of A2/B1, we investigated its colocalisation with established splicing factors and subnuclear compartments. Detergent extraction was performed on living cells prior to fixation and immunostaining. As noted above, this procedure reduced the high nuclear abundance of putatively mobile A2/B1 which normally occludes fine structural details, thus permitting a more accurate assessment of the extent of colocalisation between different proteins. In regions surrounding the nucleoli, the signal for A2/B1 overlapped with proteins recognised by the Y12 antibody and anti-5′-capped trimethylguanosine (TMG) (Fig. 4A top rows, arrows). Y12 is an autoantibody, derived from mice with a lupus-erythematosus-like syndrome, that recognises Sm proteins [44], while anti-TMG recognises processed snRNAs. Overlapping signals were also observed for U2AF^{65}, which is an early splicing factor (Fig. 4A third row, arrow). Notably, for all three antibodies, there were enriched foci in the nucleoplasm that did not colocalise with A2/B1 (Fig. 4A, arrowheads). Similarly, there was no overlap of signal with splicing factor SC-35 (Fig. 4A bottom row, arrowheads), which suggests that A2/B1 does not associate with splicing factor compartments [45].

To investigate the distribution of A2/B1 with respect to other subnuclear domains, cells were transfected with DNA expressing GFP-tagged nuclear markers, and immunostained for A2/B1. The signal for A2/B1 did not overlap with that of GFP-B23, which is a marker for the nucleolus [46]. Similarly, there were no concentrations of A2/B1 corresponding to the locations of Cajal bodies and GEMs, as indicated by GFP-coilin [47] and GFP-SMN [48], respectively (Fig. 4B, arrowheads). In contrast, the signal for A2/B1 partially coincided with that of histone 2B-GFP [49] (Fig. 4B, arrows), implying that there was colocalisation with chromatin.

As A2/B1 was found to colocalise with Sm proteins (recognised by Y12), snRNAs (recognised by anti-TMG) and U2AF^{65}, co-immunoprecipitation experiments were performed to verify the specificity of the antibodies used, and to demonstrate that the observed colocalisations were not due to cross-reactivity between the various antibodies (Supplementary data).

3.3. hnRNPs A/B associate with nucleic acids

Next, we explored the possibility that A2/B1 localisation may be dependent on its interaction with nucleic acids. HeLa cells were stained for nucleic acids and immunostained for A2/B1 to determine the extent of their colocalisation (Fig. 5A). Like histone 2B-GFP, DNA colocalised with A2/B1, particularly in the perinucleolar region (Fig. 5A, arrow). As

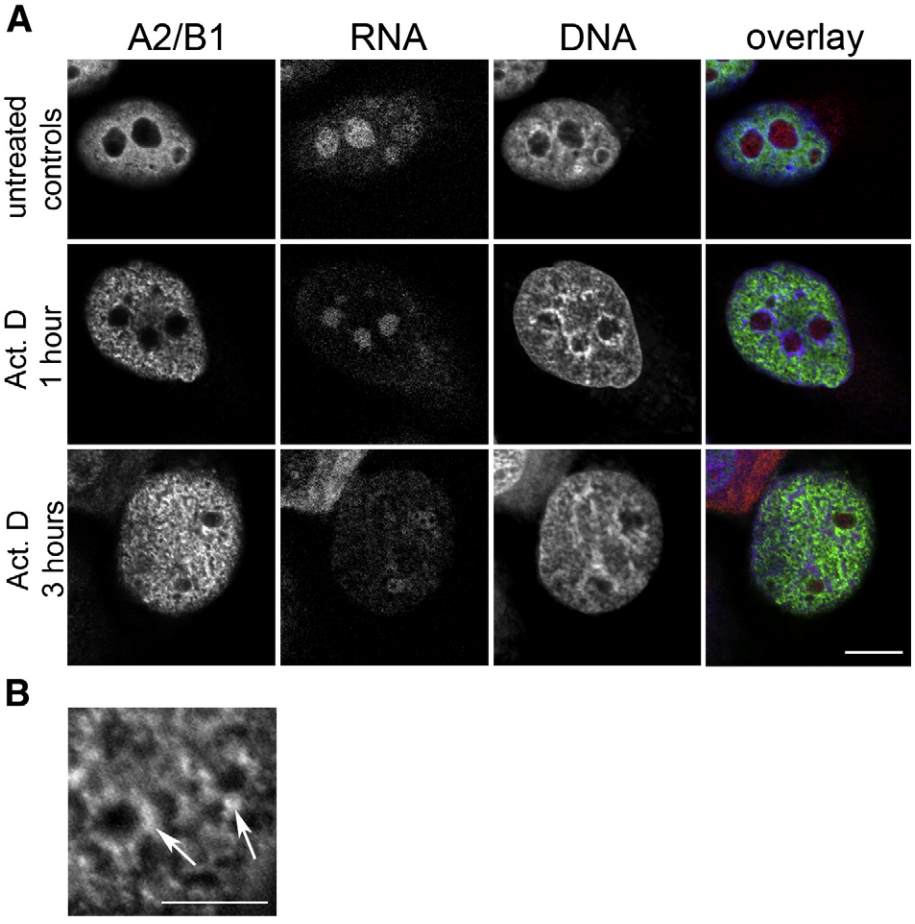

Fig. 6. Effect of transcription inhibition on A2/B1 localisation. (A) HeLa cells were treated with 5 μg/ml actinomycin D (Act. D) for 1 h or 3 h. Cells were then fixed and immunostained for A2/B1 followed by Alexafluor-488-conjugated secondary antibody (left column, green in overlay), stained for DNA using Hoechst Dye (third column, blue in overlay), and stained for RNA using Pyronin Y Dye (second column, red in overlay). Images were taken using confocal microscopy at constant settings. (B) Nucleolar remnants at higher magnification. Arrow points to the region around the nucleolar remnants where A2/B1 localisation persisted. Bar, 10 μm in (A), 5 μm in (B).

before, A2/B1 was clearly enriched surrounding, but excluded from, the nucleolus, as marked by intense staining of rRNA (Fig. 5A, arrowhead). There was also a diffuse and homogenous staining of RNA throughout the nucleoplasm outside the nucleolus.

We then looked at the effect of nuclease treatment on the localisation of A2/B1, and also U2AF^{65}, an established RNA-binding protein. Fig. 5B demonstrates the extent of nucleic acid degradation under the conditions used in the experiments. In control cells that were not treated with nucleases, staining for DNA was present throughout the nucleoplasm, and concentrated around the nucleoli. RNase A treatment completely removed RNA, while most of the DNA was removed after DNase 1 treatment and there was no discernable organisation of the DNA remnants.

HeLa cells were treated with nucleases as above and immunostained for A2/B1 and U2AF^{65}. Untreated cells displayed the same staining features as described earlier (Fig. 5C, top row). Treatment with RNase A removed most of the signal for both A2/B1 and U2AF^{65}, and enhancement of the remaining faint signals revealed that there was still considerable overlap in signal for the two proteins (Fig. 5C, middle row). This signal represents the pool of A2/B1 and U2AF^{65} that was bound to DNA and/or protein. In comparison, DNase 1 treatment removed a much smaller proportion of A2/B1 and U2AF^{65}, preserving a significant pool that was bound to RNA and/or protein (Fig. 5C, bottom row). Thus, although A2/B1 had shown a greater degree of colocalisation with DNA than with RNA in the earlier staining experiment (Fig. 5A), its localisation was more dependent on the integrity of RNA than DNA. Interestingly, the enrichment of signal around the nucleoli after DNase treatment was retained by U2AF^{65} to a greater extent than that for A2/B1 (Fig. 5C, bottom row). Thus, while the subnuclear localisation of both A2/B1 and U2AF^{65} is mostly dependent on association with RNA, there may be differences between the two proteins with respect to the nature of these associations.

The effect of RNase and DNase treatment on A1 and A3 staining was the same as that for A2/B1 (data not shown), which implies that the localisation of all three paralogues is highly dependent on RNA–protein interactions. These observations were consistent over at least 3 sets of experiments for each paralogue (data not shown).

3.4. Localisation of hnRNPs A/B is dependent on transcription activity

As A2/B1 localisation appeared to be RNA-dependent, we investigated whether altering transcription rates would affect the distribution of these proteins. After 1 h treatment with actinomycin D (which blocks the activity of RNA polymerases I, II and III), A2/B1 staining became more evenly distributed throughout the nucleoplasm while RNA levels and nucleolar size were reduced (Fig. 6A, middle row). These changes became more pronounced after actinomycin D treatment for 3 h (Fig. 6A, bottom row), but interestingly, a persistent pool of A2/B1 remained around the nucleolar remnants even when RNA levels were barely detectable (Fig. 6B, arrows). The same results were obtained for cells treated with α-amanitin, which selectively blocks RNA polymerase II (data not shown). Untreated cells showed the same staining features as described in earlier sections (Fig. 6A, top row). Similarly, the localisation of A1 and A3 was disrupted by transcription inhibition with actinomycin D (data not shown), which demonstrates that the localisation of all the hnRNPs A/B is dependent on ongoing RNA synthesis.

3.5. The hnRNPs A/B do not preferentially colocalise with transcription sites

Since we found that the localisation of hnRNPs A/B was closely associated with transcriptional activity, and as these proteins have well-established roles in the packaging of nascent mRNA [1], BrUTP (Fig. 7A–C, red) was used to label nascent transcripts in living cells in order to determine the extent of their colocalisation with the hnRNPs A/B (green). We found that the majority of transcription factories did not colocalise with the hnRNP foci. Under higher magnification, individual transcription factories [35] devoid of signal for the hnRNPs, were clearly discernable (Fig. 7D). As a negative control, cells incubated

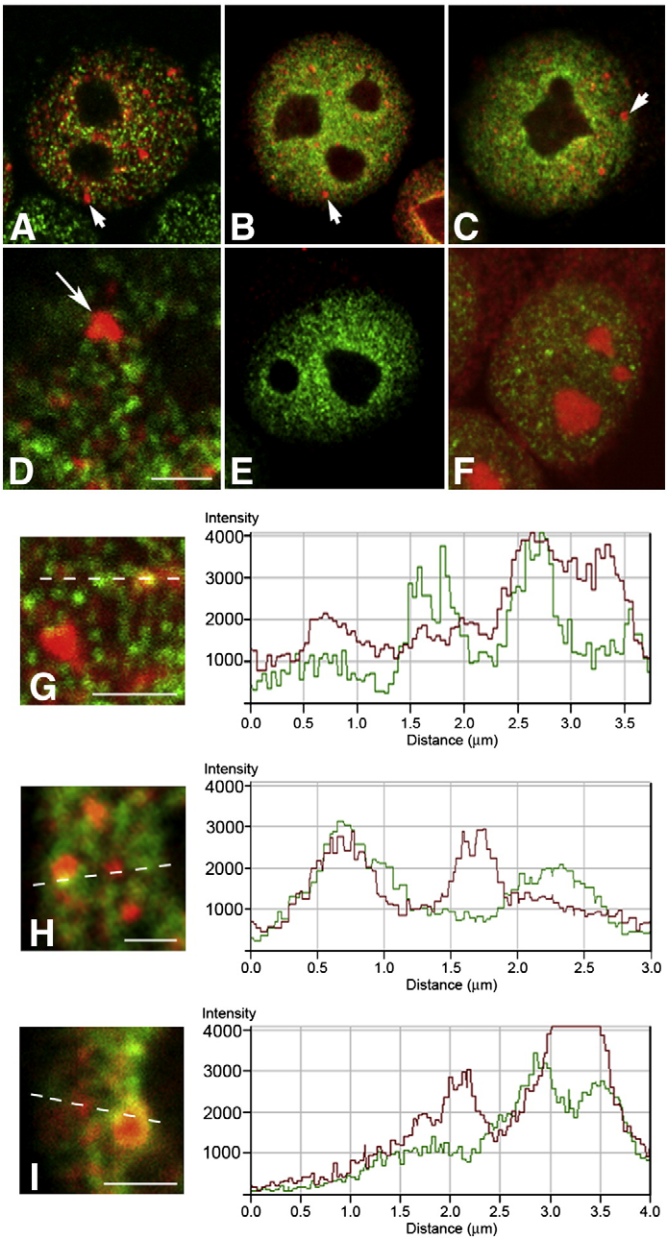

Fig. 7. hnRNPs A/B do not colocalise strongly with transcription sites. (A) HeLa cells were incubated with BrUTP to label nascent transcripts. Labelled cells were immunostained with anti-BrdU followed by anti-mouse Alexafluor-546-conjugated secondary antibody (red), and rabbit polyclonal antibodies against A1, A2/B1, A3 (A–C, respectively), followed by anti-rabbit Alexafluor-488-conjugated secondary antibody (green) and imaged by confocal microscopy. Localisation of A1 to the nuclear envelope appeared to have been perturbed by the permeabilization step in the BrUTP labelling procedure. Distinctive BrUTP-labelled foci are visible (red, short arrows). Image (D) shows, at higher magnification, a transcription factory (long arrow) that lacks overlap with A1. (E) Cells incubated with UTP in place of BrUTP were used as a negative control. (F) As a positive control, BrUTP-labelled cells were immunostained with anti-BrdU, visualised using anti-mouse Alexafluor-488-conjugated secondary antibody (green) and stained for RNA using Pyronin Y Dye (red). Images (G–I) were also obtained at higher magnification with immunodetection of hnRNP A1 (G) or A2/B1 (H and I). The adjacent profiles were obtained by scanning along the paths marked by dotted lines on the images. Bar, 2 μm in (D), and (G–I); 10 μm in (F) with the same magnification in (A–C, and E).

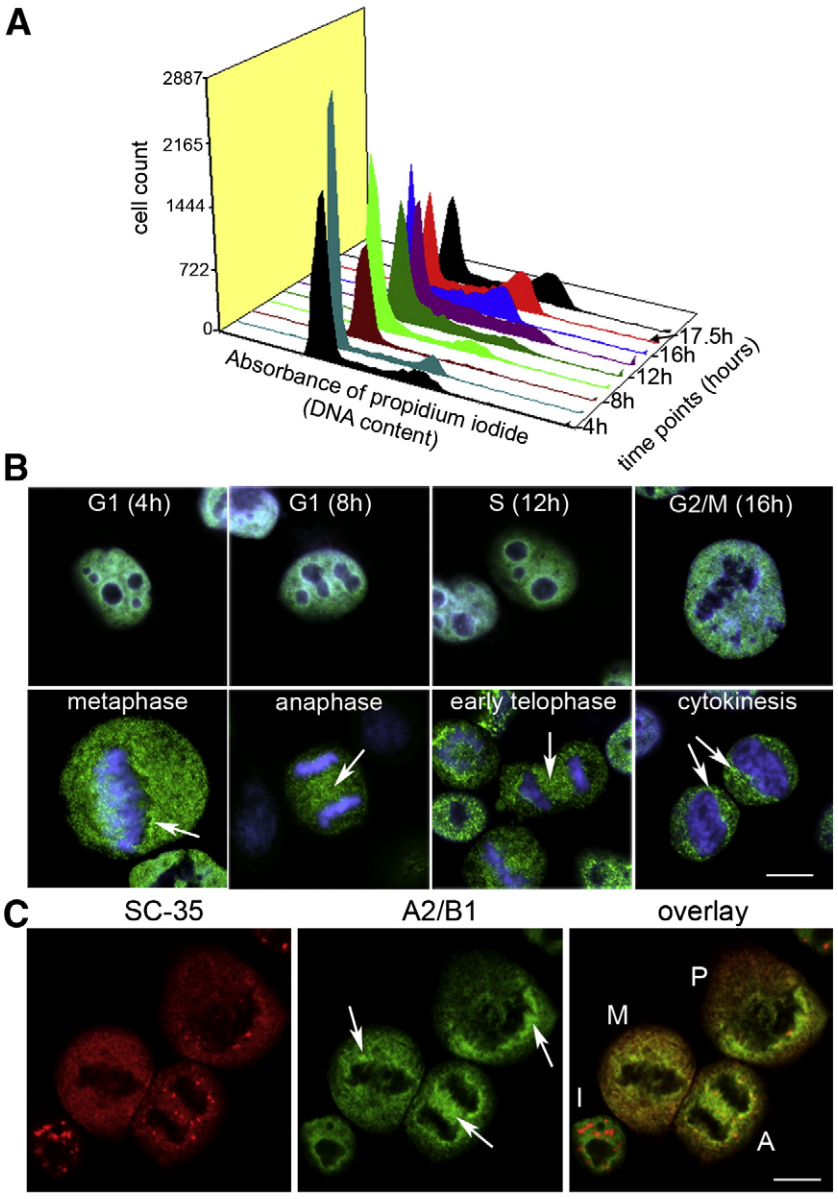

Fig. 8. Localisation of A2/B1 changes with cell cycle stages. (A) Cell synchrony of mitotic shake-off cells determined by FACS analysis. (B) HeLa cells at different stages of the cell cycle were fixed and immunostained for A2/B1 followed by anti-rabbit Alexafluor-488-conjugated secondary antibody (green) and stained for DNA with Hoechst Dye (blue). Bar, 10 μm. (C) Cells at various stages of the cell cycle (I, interphase; P, prophase; M, metaphase and A, anaphase) were immunostained for A2/B1 (green) as above, and also for SC-35 followed by anti-mouse Alexafluor-546-conjugated secondary antibody (red). Arrows point to the regions enriched for A2/B1. Bar, 10 μm.

with UTP in place of BrUTP and colabelled for A2/B1 (green) did not have any red signal for labelled nascent transcripts (Fig. 7E). As a positive control, cells labelled with BrUTP (green) and stained for RNA (red) displayed a uniform colocalisation of both signals in the nucleoplasm (Fig. 7F). There was also a small subset of transcription factories that colocated with the hnRNPs (Fig. 7G–I), but it is not possible to determine if this results from bona fide colocalisation.

3.6. Localisation of A2/B1 changes with cell cycle stage

We had noted that the pattern of localisation of A2/B1 varied between cells at different stages of the cell cycle (Fig. 3). In combination with the observation that transcription rates affect the localisation of these proteins, we further explored their distribution in synchronised cells. The cells collected by mitotic shake-off progressed through the cell cycle entering synthesis (S) and mitosis (M) phases 12 and 17.5 h, respectively, after plating out, as determined by FACS analysis (Fig. 8A). These results are in agreement with mitotic shake-off cell cycle characteristics for HeLa cells [50]. Cell cycle stages were then assigned to the immunofluorescent data time points. The perinucleolar enrichment of A2/B1 was maintained throughout interphase (Fig. 8B (G1-S)) and began dispersing in early mitosis (Fig. 8B (G2/M)). During mitosis, the pattern of A2/B1 staining was generally diffuse, although there appeared to be some regional concentrations of staining (Fig. 8B (bottom row), C, arrows). By comparison, the distribution of SC-35 was more homogeneous than the A2/B1 distribution at metaphase (Fig. 8C).

4. Discussion

Sequence comparisons suggest that hnRNPs A1, A2/B1 and A3 are derived from a common ancestral gene sequence [51]. These proteins are highly conserved across a variety of eukaryotic species and share overlapping functions in a number of cellular pathways. Simultaneous suppression of multiple paralogues resulted in a greater retardation of

cell proliferation than suppression of individual paralogues, which indicates that there is functional compensation by the other paralogues when only one is suppressed [2,4,52]. Mouse hepatitis virus (MHV) replication still takes place in the CB3 cell line, which does not express A1, because the other paralogues can fill its role in RNA synthesis [53]. Both A1 and A2/B1 have well-documented and highly similar roles in RNA processing [1], in particular splicing [54]. This apparent functional redundancy may represent a "backup" system to ensure that these vital cellular processes can take place even if one of the paralogues is non-functional.

Although the hnRNPs A/B share a high degree of sequence identity and structural similarity, the subnuclear localisation of A1 differed markedly and consistently from that of A2/B1 and A3 (Fig. 3). A1 was preferentially localised at the nuclear envelope, whereas A2/B1 and A3 were widely distributed but concentrated near nucleoli. All three proteins possess the same overall organisation of two N-terminal RNA recognition motifs (RRMs) joined by a short linker, followed by a C-terminal glycine-rich domain (GRD) [55]. The GRD of A3 is more similar in sequence to that of A2/B1 than A1, whereas the converse is true for the RRMs [37]. The subnuclear distribution of A3 resembles that of A2/B1 more closely than that of A1 throughout interphase, metaphase and anaphase, which may indicate that the interactions regulating the localisation of these proteins may be largely determined by the GRD.

The differential localisation of the hnRNPs A/B may have functional implications. Al has been detected throughout DNA replication bodies by electron microscopy, and its presence has been attributed to the colocalisation of replication and transcription [56]. Replicating chromatin distributes to the nuclear periphery and is largely absent from the internal nucleoplasmic volume at the later stages of S phase [57]. Thus, the immunostaining pattern of A1 could reflect its association with late replicating DNA. Hence, the differences in the distribution of A1 versus A2 and A3 may result from their involvement in distinct sets of nuclear processes.

In addition, our results indicate that localisation of the hnRNPs A/B is highly dependent on interactions with RNA (Fig. 5). Although colocalisation of transcription factories (which contain the majority of nascent extranucleolar transcripts [58]) with hnRNP A/B foci was rarely observed, it is possible that newly transcribed pre-mRNAs interact on a short timescale with the mobile pool of nucleoplasmic hnRNPs [59]. Additionally, many of hnRNPs A/B foci appeared to be within a micron of a transcription factory and therefore could also be available for interaction with pre-mRNAs shortly after their transcription (Fig. 7). The importance of interactions between RNA and the hnRNPs is reinforced by the observation that the focal distribution of the hnRNPs A/B was abolished following inhibition of transcription (Fig. 6), suggesting that the hnRNPs A/B interact with transcripts some time after their synthesis.

The hnRNPs A/B recognise specific motifs in various mRNAs [19,37,60,61], while different sequences in transcripts bind different sets of hnRNPs [62]. Furthermore, A1 and A2/B1 have dissimilar affinities for newly spliced AdML and β-globin transcripts [63]. In addition, hnRNPs A/B act as splicing silencers [15–19], which implies that they would only be found on mRNAs undergoing exonic skipping. Given that the hnRNPs A/B interact with mRNAs in a sequence-specific manner, studies that look at pools of RNPs are unlikely to be able to elucidate the true nature of these interactions.

The partial colocalisation of A2/B1 with splicing factors $U2AF^{65}$, snRNA and Sm proteins (Fig. 4) provides further support for its role in splicing. This colocalisation was most prominent in the perinucleolar region. There is now mounting evidence that the nucleolus may be involved in the assembly of small nuclear RNPs (snRNPs), which are precursors of spliceosomes [64]. Proteomic analyses of nucleoli have also consistently identified a high proportion of proteins (about 20%) that are involved in mRNA metabolism [21]. In combination with our findings, this suggests that elevated levels of mRNA processing, including the early stages of splicing, may take place in the perinucleolar region.

snRNPs are assembled in the cytoplasm and imported back into the nucleus where they undergo maturation in Cajal bodies. They then can be stored in splicing factor compartments before incorporation into spliceosomes to catalyze splicing [33,34]. Interestingly, A2/B1 does not colocalise with SC-35, a marker for splicing factor compartments, or with Cajal bodies (and closely related structures, GEMs), as marked by concentrations of snRNAs, coilin or SMN (Fig. 4). This further suggests that the association of A2/B1 with snRNP components occurs only in the spliceosome. However, at the level of resolution employed in our experiments, the possibility of additional non-spliceosomal functions at these locations cannot be precluded.

During mitosis, many subnuclear compartments are relocalised as the nucleus undergoes structural reorganisation. During prophase and metaphase, splicing factors such as SC-35 and the snRNPs diffuse throughout the cell body, before reassembling into Cajal bodies and splicing factor compartments in late anaphase [65]. Similarly, we found that the distribution of A2/B1 changed from a perinucleolar enrichment during interphase to a more diffuse pattern throughout mitosis, although there were some regional concentrations of A2/B1 staining (Fig. 8). Since the perinucleolar localisation of A2/B1 is dependent on ongoing transcription (Fig. 6), these transitions may be a consequence of the inhibition of transcription that occurs during mitosis.

In summary, our results demonstrate that the hnRNPs A/B have distinct subnuclear localisation patterns that are spatially and temporally regulated. The distribution of A1 differs greatly from that of A2/B1 and A3, and this localisation is maintained primarily by interactions with RNA. The presence and absence of hnRNPs A/B from particular subnuclear compartments may be related to their involvement in specific stages of nuclear processes such as DNA replication and splicing. Our findings suggest that while the hnRNPs A/B retain a high degree of structural homology and have closely related roles in processes such as RNA packaging, they have diverged to become functionally distinct in other aspects. It will be of great interest to further elucidate the differential contribution of these paralogues to the many nuclear pathways in which they are involved.

Acknowledgments

This work was supported by a grant to R.S. and J.A.R. from the Australian National Health and Medical Research Council. We thank Dr. G. Osborne (University of Queensland) for assistance with FACS analysis, Dr. J. E. Cassanova (University of Virginia), for the kind gift of plasmids, G. Korza (University of Connecticut) for assistance with the B104 cell experiments, Dr. R. de las Heras (The University of Queensland) for isolating the hippocampal neurons, and Dr N.A. Saunders (The University of Queensland) for supplying primary keratinocytes.

Appendix A. Supplementary data

Supplementary data associated with this article can be found, in the online version, at doi:10.1016/j.bbamcr.2008.05.021.

References

[1] G. Dreyfuss, V.N. Kim, N. Kataoka, Messenger-RNA-binding proteins and the messages they carry, Nat. Rev. Mol. Cell Biol. 3 (2002) 195–205.
[2] C. Patry, B. Lemieux, R.J. Wellinger, B. Chabot, Targeting heterogeneous nuclear ribonucleoparticule A1 and A2 proteins by RNA interference promotes cell death in transformed but not in normal mouse cell lines, Mol. Cancer Ther. 3 (2004) 1193–1199.
[3] S. Kwon, E. Barbarese, J.H. Carson, The *cis*-acting RNA trafficking signal from myelin basic protein mRNA and its cognate *trans*-acting ligand hnRNP A2 enhance cap-dependent translation, J. Cell Biol. 147 (1999) 247–256.
[4] Y. He, M.A. Brown, J.A. Rothnagel, N.A. Saunders, R. Smith, Roles of heterogeneous nuclear ribonucleoproteins A and B in cell proliferation, J. Cell Sci. 118 (2005) 3173–3183.

[5] S. Guil, J.C. Long, J.F. Caceres, hnRNP A1 relocalisation to the stress granules reflects a role in the stress response, Mol. Cell. Biol. 26 (2006) 5744–5758.
[6] S. Guil, J.F. Caceres, The multifunctional RNA-binding protein hnRNP A1 is required for processing of miR-18a, Nature Struct. Mol. Biol. 14 (2007) 591–596.
[7] J.F. Caceres, S. Stamm, D.M. Helfman, A.R. Krainer, Regulation of alternative splicing *in vivo* by overexpression of antagonistic splicing factors, Science 265 (1994) 1706–1709.
[8] A. Mayeda, A.R. Krainer, Regulation of alternative pre-mRNA splicing by hnRNP-A1 and splicing factor SF2, Cell 68 (1992) 365–375.
[9] I. Listerman, A.K. Sapra, K.M. Neugebauer, Cotranscriptional coupling of splicing factor recruitment and precursor messenger RNA splicing in mammalian cells, Nature Struct. Mol. Biol. 13 (2006) 815–822.
[10] K. Moran-Jones, L. Wayman, D.D. Kennedy, R.R. Reddel, S. Sara, M.J. Snee, R. Smith, hnRNP A2, a potential ssDNA/RNA molecular adapter at the telomere, Nucleic Acids Res. 33 (2005) 486–496.
[11] E. Tanaka, H. Fukuda, K. Nakashima, N. Tsuchiya, H. Seimiya, H. Nakagama, HnRNP A3 binds to and protects mammalian telomeric repeats *in vitro*, Biochem. Biophys. Res. Commun. 358 (2007) 608–614.
[12] Q.S. Zhang, L. Manche, R.M. Xu, A.R. Krainer, hnRNP A1 associates with telomere ends and stimulates telomerase activity, RNA 12 (2006) 1116–1128.
[13] P.-R. Huang, S-T. Tsai, K-H. Hieh, T-C.V. Wang, Heterogeneous nuclear ribonucleoprotein A3 binds single-stranded telomeric DNA and inhibits telomerase extension *in vitro*, Biochim. Biophys. Acta 1783 (2008) 193–202.
[14] Q. Chai, L. Zheng, M. Zhou, J.J. Turchi, B.H. Shen, Interaction and stimulation of human FEN-1 nuclease activities by heterogeneous nuclear ribonucleoprotein A1 in alpha-segment processing during Okazaki fragment maturation, Biochemistry 42 (2003) 15045–15052.
[15] Q. Sun, A. Mayeda, R.K. Hampson, A.R. Krainer, F.M. Rottman, General splicing factor SF2/ASF promotes alternative splicing by binding to an exonic splicing enhancer, Genes Dev. 7 (1993) 2598–2608.
[16] M. Caputi, A. Mayeda, A.R. Krainer, A.M. Zahler, hnRNP A/B proteins are required for inhibition of HIV-1 pre-mRNA splicing, EMBO J. 18 (1999) 4060–4067.
[17] F. del Gatto-Konczak, M. Olive, M. Gesnel, R. Breathnach, hnRNP A1 recruited to an exon in vivo can function as an exon splicing silencer, Mol. Cell. Biol. 19 (1999) 251–260.
[18] P.S. Bilodeau, J.K. Domsic, A. Mayeda, A.R. Krainer, C.M. Stoltzfus, RNA splicing at human immunodeficiency virus type 1 3′ splice site A2 is regulated by binding of hnRNP A/B proteins to an exonic splicing silencer element, J. Virol. 75 (2001) 8487–8497.
[19] J.K. Domsic, Y.B. Wang, A. Mayeda, A.R. Krainer, C.M. Stoltzfus, Human immunodeficiency virus type 1 hnRNP A/B-dependent exonic splicing silencer ESSV antagonizes binding of U2AF65 to viral polypyrimidine tracts, Mol. Cell. Biol. 23 (2003) 8762–8772.
[20] J. Andersen, C. Lyon, A. Fox, A. Leung, Y. Lam, H. Steen, M. Mann, A.I. Lamond, Directed proteomic analysis of the human nucleolus, Curr. Biol. 12 (2002) 1–11.
[21] Y. Coute, J. Burgess, J. Diaz, C. Chichester, F. Lisacek, A. Greco, J. Sanchez, Deciphering the human nucleolar proteome, Mass Spectrometry Reviews 25 (2006) 215–234.
[22] H. Kamma, H. Horiguchi, L.L. Wan, M. Matsui, M. Fujiwara, M. Fujimoto, T. Yazawa, G. Dreyfuss, Molecular characterization of the hnRNP A2/B1 proteins: tissue-specific expression and novel isoforms, Exp. Cell Res. 246 (1999) 399–411.
[23] D. Vautier, P. Chesne, C. Cunha, A. Calado, J.P. Renard, M. Carmo-Fonseca, Transcription-dependent nucleocytoplasmic distribution of hnRNP A1 protein in early mouse embryos, J. Cell Sci. 114 (2001) 1521–1531.
[24] J. Deckert, K. Hartmuth, D. Boehringer, N. Behzadnia, C.L. Will, B. Kastner, H. Stark, H. Urlaub, R. Luhrmann, Protein composition and electron microscopy structure of affinity-purified human spliceosomal B complexes isolated under physiological conditions, Mol. Cell. Biol. 26 (2006) 5528–5543.
[25] K. Hartmuth, H. Urlaub, H. Vornlocher, C. Will, M. Gentzel, M. Wilm, R. Luhrmann, Protein composition of human prespliceosomes isolated by a tobramycin affinity-selection method, Proc. Natl. Acad. Sci. USA 99 (2002) 16719–16724.
[26] M. Jurica, L. Licklider, S. Gygi, N. Grigorieff, M. Moore, Purification and characterization of native spliceosomes suitable for three-dimensional structural analysis, RNA 8 (2002) 426–439.
[27] E. Makarov, O. Makarova, H. Urlaub, M. Gentzel, C. Will, M. Wilm, R. Luhrmann, Small nuclear ribonucleoprotein remodeling during catalytic activation of the spliceosome, Science 298 (2002) 2205–2208.
[28] J. Rappsilber, U. Ryder, A.I. Lamond, M. Mann, Large-scale proteomic analysis of the human splicesome, Genome Res. 12 (2002) 1231–1245.
[29] Z. Zhou, L. Licklider, S. Gygi, R. Reed, Comprehensive proteomic analysis of the human spliceosome, Nature 419 (2002) 182–185.
[30] T. Misteli, Beyond the sequence: cellular organization of genome function, Cell 128 (2007) 787–800.
[31] K.E. Handwerger, J.G. Gall, Subnuclear organelles: new insights into form and function, Trends Cell Biol. 16 (2006) 19–26.
[32] T. Misteli, J.F. Caceres, J.Q. Clement, A.R. Krainer, M.F. Wilkinson, D.L. Spector, Serine phosphorylation of SR proteins is required for their recruitment to sites of transcription *in vivo*, J. Cell Biol. 143 (1998) 297–307.
[33] J.E. Sleeman, A.I. Lamond, Newly assembled snRNPs associate with coiled bodies before speckles, suggesting a nuclear snRNP maturation pathway, Curr. Biol. 9 (1999) 1065–1074.
[34] J.S. Yong, L.L. Wan, G. Dreyfuss, Why do cells need an assembly machine for RNA–protein complexes? Trends Cell Biol. 14 (2004) 226–232.
[35] P.R. Cook, The organization of replication and transcription, Science 284 (1999) 1790–1795.
[36] P.R. Cook, Predicting three-dimensional genome structure from transcriptional activity, Nat. Genet. 32 (2002) 347–352.
[37] A.S.W. Ma, K. Moran-Jones, J. Shan, T.P. Munro, M.J. Snee, K.S. Hoek, R. Smith, Heterogeneous nuclear ribonucleoprotein A3, a novel RNA trafficking response element-binding protein, J. Biol. Chem. 277 (2002) 18010–18020.
[38] A.H. Fox, C.S. Bond, A.I. Lamond, P54nrb forms a heterodimer with PSP1 that localises to paraspeckles in an RNA-dependent manner, Mol. Biol. Cell 16 (2005) 5304–5315.
[39] J. Andersen, Y. Lam, A. Leung, S. Ong, C. Lyon, A.I. Lamond, M. Mann, Nucleolar proteome dynamics, Nature 433 (2005) 77–83.
[40] C. Elbi, T. Misteli, G.L. Hager, Recruitment of dioxin receptor to active transcription sites, Mol. Biol. Cell 13 (2002) 2001–2015.
[41] A. van Opstal, J. Boonstra, Inhibitors of phosphatidylinositol 3-kinase activity prevent cell cycle progression and induce apoptosis at the M/G1 transition in CHO cells, Cell. Mol. Life Sci. 63 (2006) 220–228.
[42] G.E. Moore, S.B. Merrick, L.K. Woods, N.M. Arabasz, Human squamous-cell carcinoma cell line, Cancer Res. 35 (1975) 2684–2688.
[43] D.J. Anderson, M.W. Hetzer, Nuclear envelope formation by chromatin-mediated reorganization of the endoplasmic reticulum, Nat. Cell Biol. 9 (2007) 1160–1166.
[44] E. Lerner, M. Lerner, C. Janeway, J. Steitz, Monoclonal antibodies to nucleic acid-containing cellular constituents — probes for molecular-biology and autoimmune disease, Proc. Natl. Acad. Sci. U. S. A. 78 (1981) 2737–2741.
[45] I. Melcak, S. Cermanova, K. Jirsova, K. Koberna, J. Malinsky, I. Raska, Nuclear pre-mRNA compartmentalization: trafficking of released transcripts to splicing factor reservoirs, Mol. Biol. Cell 11 (2000) 497–510.
[46] D.Y. Chen, S. Huang, Nucleolar components involved in ribosome biogenesis cycle between the nucleolus and nucleoplasm in interphase cells, J. Cell Biol. 153 (2001) 169–176.
[47] M.D. Hebert, A.G. Matera, Self-association of coilin reveals a common theme in nuclear body localisation, Mol. Biol. Cell 11 (2000) 4159–4171.
[48] J.E. Sleeman, P. Ajuh, A.I. Lamond, snRNP protein expression enhances the formation of Cajal bodies containing p80-coilin and SMN, J. Cell Sci. 114 (2001) 4407–4419.
[49] A. Dey, J. Ellenberg, A. Farina, A.E. Coleman, T. Maruyama, S. Sciortino, J. Lippincott-Schwartz, K. Ozato, A bromodomain protein, MCAP, associates with mitotic chromosomes and effects, G(2)-to-M transition, Mol. Cell. Biol. 20 (2000) 6537–6549.
[50] M.L. Whitfield, G. Sherlock, A.J. Saldanha, J.I. Murray, C.A. Ball, K.E. Alexander, J.C. Matese, C.M. Perou, M.M. Hurt, P.O. Brown, D. Botstein, Identification of genes periodically expressed in the human cell cycle and their expression in tumors, Mol. Biol. Cell 13 (2002) 1977–2000.
[51] A.A. Akindahunsi, A. Bandiera, G. Manzini, Vertebrate 2xRBD hnRNP proteins: a comparative analysis of genome, mRNA and protein sequences, Comp. Biol. Chem. 29 (2005) 13–23.
[52] C. Patry, L. Bouchard, P. Labrecque, D. Gendron, B. Lemieux, J. Toutant, E. Lapointe, R. Wellinger, B. Chabot, Small interfering RNA-mediated reduction in heterogeneous nuclear ribonucleoparticule A1/A2 proteins induces apoptosis in human cancer cells but not in normal mortal cell lines, Cancer Res. 63 (2003) 7679–7688.
[53] S.T. Shi, G.Y. Yu, M.M.C. Lai, Multiple type A/B heterogeneous nuclear ribonucleoproteins (hnRNPs) can replace hnRNP A1 in mouse hepatitis virus RNA synthesis, J. Virol. 77 (2003) 10584–10593.
[54] A. Mayeda, S.H. Munroe, J.F. Caceres, A.R. Krainer, Function of conserved domains of hnRNP A1 and other hnRNP A/B proteins, EMBO J. 13 (1994) 5483–5495.
[55] A. Kumar, K.R. Williams, W. Szer, Purification and domain structure of core hnRNP proteins A1 and A2 and their relationship to single-stranded DNA-binding proteins, J. Biol. Chem. 261 (1986) 11266–11273.
[56] A.A. Philimonenko, Z. Hodny, D.A. Jackson, P. Hozak, The microarchitecture of DNA replication domains, Histochem. Cell Biol. 125 (2006) 103–117.
[57] J. Ferreira, G. Paolella, C. Ramos, A.I. Lamond, Spatial organization of large-scale chromatin domains in the nucleus: a magnified view of single chromosome territories, J. Cell Biol. 139 (1997) 1597–1610.
[58] D. Jackson, F. Iborra, E. Manders, P. Cook, Numbers and organization of RNA polymerases, nascent transcripts, and transcription units in HeLa nuclei, Mol. Biol. Cell 9 (1998) 2698.
[59] F.S. Fay, K.L. Taneja, S. Shenoy, L. Lifshitz, R.H. Singer, Quantitative digital analysis of diffuse and concentrated nuclear distributions of nascent transcripts, SC35 and poly(A), Exp. Cell Res. 231 (1997) 27–37.
[60] K.S. Hoek, G.J. Kidd, J.H. Carson, R. Smith, hnRNP A2 selectively binds the cytoplasmic transport sequence of myelin basic protein mRNA, Biochemistry 37 (1998) 7021–7029.
[61] S. Hutchison, C. LeBel, M. Blanchette, B. Chabot, Distinct sets of adjacent heterogeneous nuclear ribonucleoprotein (hnRNP) A1/A2 binding sites control 5′ splice site selection in the hnRNP A1 mRNA precursor, J. Biol. Chem. 277 (2002) 29745–29752.
[62] M. Bennett, S. Pinol-Roma, D. Staknis, G. Dreyfuss, R. Reed, Differential binding of heterogeneous nuclear ribonucleoproteins to mRNA precursors prior to spliceosome assembly *in vitro*, Mol. Cell. Biol. 12 (1992) 3165–3175.
[63] C. Merz, H. Urlaub, C.L. Will, R. Luhrmann, Protein composition of human mRNPs spliced *in vitro* and differential requirements for mRNP protein recruitment, RNA 13 (2007) 116–128.
[64] S.A. Gerbi, A.V. Borovjagin, T.S. Lange, The nucleolus: a site of ribonucleoprotein maturation, Curr. Opin. Cell Biol. 15 (2003) 318–325.
[65] B.J. Blencowe, Splicing regulation: the cell cycle connection, Curr. Biol. 13 (2003) R149–R151.